Kinetic Energy Release from Reverse Critical Energy

Bull. Korean Chem. Soc. **1994**, *Vol. 15, No. 3* 241

10. Calculations were performed using the *Structure Determination Package Programs* written by Frenz, B. A.; Okaya, Y. Enraf-Nonius, Netherlands, 1987.
11. *International Tables for X-ray Crystallography*, Kynoch: Birmingham, England, 1974; Vol. II, p 132.
12. Koh, K. N.; Kim, U. S.; Kim, D. S.; Kim, Y. *Bull. Korean Chem. Soc.* **1991**, *12*, 178.
13. Jang, S. B.; Kim, Y. *J. Korean Chem. Soc.* **1993**, *37*, 191.
14. Heo, N. H.; Seff, K. *J. Am. Chem. Soc.* **1987**, *109*, 7986.
15. Heo, N. H.; Seff, K. *J. Chem. Soc. Chem. Commun.* **1987**, 1225.
16. Doyle, P. A.; Turner, P. S. *Acta Crystallogr. Sect. A.: Cryst. Phys. Diff. Theor. Gen. Crystallogr.* **1968**, *24*, 390.

17. *International Tables for X-ray Crystallography*, Kynoch: Birmingham, England. 1974; Vol. IV, p 73.
18. Reference 17, p 149.
19. *Handbook of Chemistry and Physics*, 70th ed.; Chemical Rubber Co.: Cleveland, 1989/1990; p F-187.
20. Song, S. H.; Kim, Y.; Seff, K. *J. Phys. Chem.* **1991**, *95*, 9919.
21. Song, S. H.; Ph. D. Thesis, Pusan National University, **1991**.
22. Blackwell, C. S.; Pluth, J. J.; Smith, J. V. *J. Phys. Chem.* **1985**, *89*, 4420.
23. Reference 19, p F-157.

Determination of the Kinetic Energy Release Originating from the Reverse Critical Energy in Unimolecular ion Dissociation

In Chul Yeh, Tae Geol Lee, and Myung Soo Kim*

Department of Chemistry and Research Institute of Molecular Sciences
Seoul National University Seoul 151-742
Received October 29, 1993

A method has been developed to estimate the kinetic energy release originating from the reverse critical energy in unimolecular ion dissociation. Contribution from the excess energy was estimated by RRKM theory, the statistical adiabatic model and the modified phase space calculation. This was subtracted from the experimental kinetic energy release distribution (KERD) via deconvolution. The present method has been applied to the KERDs in H_2 loss from $C_6H_6^{+}$ and HF loss from $CH_2CF_2^{+}$. In the present formalism, not only the energy in the reaction coordinate but also the energy in some transitional vibrational degrees of freedom at the transition state is thought to contribute to the experimental kinetic energy release. Details of the methods for treating the transitional modes are found not to be critical to the final outcome. For a reaction with small excess energy and large reverse critical energy, KERD is shown to be mainly governed by the reverse critical energy.

Introduction

There have been considerable interests in the energy disposal in the product regions of unimolecular reactions.[1-4] Statistical models such as the phase space theory[5-8] and the flexible transition state theory[3] have provided good descriptions of the product state distributions for a number of unimolecular reactions going through loose transition states without significant reverse critical energies.[3,5,7,12] In a more general unimolecular reaction with a significant reverse critical energy, there are two distinct components of the internal energy available for partitioning in the products. These are the non-fixed excess energy at the transition state and the reverse critical energy.[1,2,13,14] In this case, further assumptions concerning the dynamics in the exit channel are needed to formulate the energy partitioning within the statistical framework.[15,16] The simplest of such assumptions is, for example, to assign the entire reverse critical energy to the relative translation of the products.[15-17] In most of the cases,

however, the experimental kinetic energy release is substantially smaller than the value evaluated under the above assumption.[13,18] This means that some of the reverse critical energy is converted into product vibrations and rotations.[19]

In unimolecular ion dissociation, discussion on the energy partitioning has been limited to the magnitude of the product relative translation.[13,14] This is mainly due to the difficulty in the measurement of vibrational and rotational states of products. Various mass spectrometric techniques have been developed to measure the average of the kinetic energy release (KER) or its distribution (KERD).[13] The average KER or KERD thus obtained is used as a probe in the study of ion structure and fragmentation mechanism.[14] In particular, the fractions of the reverse critical energy released as the relative translational energy of the products in multi-centered elimination reactions have been though to be of diagnostic value in the assignment of transition state geometries.[13,14]

It has long been recognized that the kinetic energy released from the reverse critical energy depends upon the detailed energetics and dynamics of the reaction and is intrinsic to the particular process.[13] A practical difficulty in the meas-

---

*To whom correspondence should be addressed.

urement of this quantity arises from the fact that the non-fixed excess energy at the transition state also contributes to the kinetic energy release.[13,14] There have been considerable discussions on the role of the two energy terms, the excess energy and the reverse critical energy, in the energy partitioning in the products.[1,2,13,14] However, a definite conclusion has not been reached yet on whether the two energy terms should be treated differently or not.

As an extension of our effort to understand the kinetics and dynamics of multi-centered elimination reaction,[18] an attempt is made in this work to extract KERD originating from the reverse critical energy. The method is applied to elimination reactions with small (reaction (1)) and large (reaction (2)) reverse barriers.

$$C_6H_6^{+\cdot} \rightarrow C_6H_4^{+\cdot} + H_2 \tag{1}$$

$$CH_2CF_2^{+\cdot} \rightarrow CHCF^+ + HF \tag{2}$$

Experimental

Laboratory kinetic energy profile of a unimolecular ion dissociation was obtained by mass-analyzed ion kinetic energy spectrometry (MIKES)[13] using a VG ZAB-E double focusing mass spectrometer with reversed geometry (VG Analytical Ltd., Manchester, UK). Schematic diagram of a cell assembly located near the intermediate focal point of the instrument, which is normally used as a collision cell, was shown elsewhere.[20,21] Ions were generated by 70 eV electron ionization and were accelerated to 8 keV. Ion source temperature was maintained at 180°C. Molecular ion was selected by adjusting the magnetic field of the magnetic analyzer. Among the unimolecular dissociation products generated in the second field-free region of the instrument, namely, the region between the magnetic and electric sectors, only those generated inside the cell assembly were separated by floating the cell at high voltage.[22] This was to observe dissociation occurring within a well-defined narrow time window. Time of dissociation, namely the time interval between the formation of the molecular ion in the source and its arrival at the center of the cell assembly, was estimated by ion-optical calculation. With the ion accelerating voltage of 8 kV and -1031 and -2860 V of the applied voltage on the cell, they were about 20.5 ± 2.0 μsec for $CH_2CF_2^+$ and 22.6 ± 2.0 μsec for $C_6H_6^{+\cdot}$, respectively. Ion kinetic energy profile was scanned repetitively and averaged to obtain data of very high quality.

Principle of the Method

It has been suggested by previous investigators that the excess energy at the transition state and the reverse barrier contribute independently to the kinetic energy release.[13,14] Thus, two kinetic energy release terms originating from these energy components have been simply added to account for the experimental kinetic energy release.[13,14] Hence, the total kinetic energy release T is usually written as

$$T = T_\alpha + T_r \tag{3}$$

Here, T_α is the contribution to the kinetic energy release from the excess energy at the transition state and T_r is that from the reverse barrier. In most of the ion decomposition

reactions, however, the kinetic energy release does not appear as a single value, but has a certain distribution. A more general but equally speculative assumption will be made in the present work to take these distributions into account. Namely, it will be assumed that two kinetic energy release distributions (KERD), $n_r(T)$ and $n_\alpha(T)$, originate from the reverse barrier (E_o) and the excess energy (E_α), respectively, and that the two contribute to the overall KERD independently. Under this assumption, the probability density for the case in which the reverse barrier and the excess energy contribute t and $T-t$, respectively, to the overall kinetic energy release T becomes $n_\alpha(T-t)n_r(t)$. Then, summing over t results in the overall KERD. Namely,

$$n(T) = \int_o^T n_\alpha(T-t)n_r(t)dt \tag{4}$$

where $n_\alpha(T) = 0$ where $T < 0$ or $T > E_\alpha$. Since $n_r(T)$ is physically meaningful only when $0 \le T \le E_o$ and vanishes outside of this region, Eqn. (4) can be written as a convolution integral.[24]

$$n(T) = \int_{-\infty}^{\infty} n_\alpha(T-t)n_r(t)dt \tag{5}$$

Hence, knowing two of the KERD functions, the third can be evaluated by convolution or deconvolution using the fast Fourier transform technique.[23] The main practical obstacle in the evaluation of $n_r(T)$ lies in the fact that $n_\alpha(T)$ is not known, which requires the second major assumption of the present procedure.

The previous assumption that $n_\alpha(T)$ and $n_r(T)$ can be treated separately presupposes that the exact dynamics along the exit channel would not have profound influence on the partitioning of the excess energy. Such a situation suggests several means to estimate $n_\alpha(T)$ within the framework of the existing statistical methods. Three different approaches have been used here to estimate $n_\alpha(T)$ and the resulting $n_r(T)$'s are compared. In the first method based on Rice-Ramsperger-Kassel-Marcus (RRKM) theory,[24,25] $n_\alpha(T)$ is taken as the energy distribution along the reaction coordinate at the transition state. Namely,

$$n_\alpha(T) \propto \rho^\ddagger(E_\alpha - T) \tag{6}$$

where $\rho^\ddagger(E_\alpha - T)$ represents the density of states at the energy $E_\alpha - T$ in degrees of freedom other than the reaction coordinate.[17,26] The second method is based on the statistical adiabatic model developed by Marcus[15,16] to take into account the disposal of the excess energy of the bending vibrations in unimolecular reactions with the tight transition states. In the actual calculation, an alternative formalism developed by Chesnavich and Bowers[8,26] from the perspective of the reverse reaction has been adopted. Namely,

$$n_\alpha(T; E_\alpha, J) \propto F^\ddagger(E_\alpha, J, T) \tag{7}$$

where $F^\ddagger(E_\alpha, J, T)$ is the angular momentum (J) conserved microcanonical flux of the reverse reaction at fixed translational energy T.[8] Further details on the mathematical expressions can be found in appendix B 4 of ref. 8 and ref. 26. The third approach is related to the modified phase space model presented previously.[18] The system degrees of freedom are divided into two groups, one consisting of the conserved

Kinetic Energy Release from Reverse Critical Energy

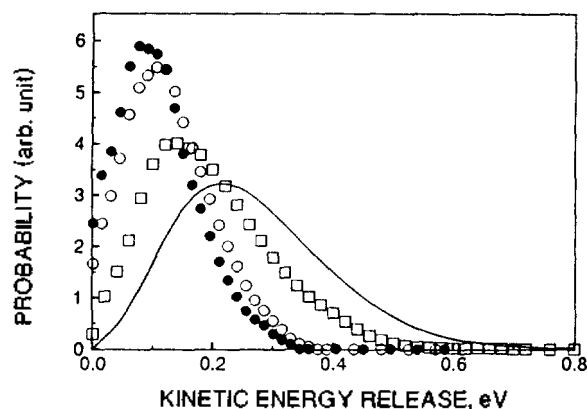*Bull. Korean Chem. Soc.* 1994, *Vol. 15, No. 3* 243

Figure 1. Solid line represents the experimental KERD in reaction (1). Symbols represent $n_r(T)$ estimated by the method described in the text. RRKM theory (□), the statistical adiabatic model (●), and the modified phase space calculation (○) have been used to estimate $n_{ex}(T)$ needed for the deconvolution of the experimental KERD.

modes and the other consisting of transitional modes and the reaction coordinate. The distribution of the energy stored in the second group at the tight transition state is evaluated according to the method described previously.[18] This energy is redistributed to the corresponding vibrational, rotational, and translational degrees of freedom via phase space calculation at the orbiting transition state. The only difference from the method described in the previous work is to exclude the reverse critical energy in the phase space calculation of KERD.

The internal energy distribution for $C_6H_6^{+\cdot}$ molecular ion dissociating within the instrumentally defined time window has been reported already.[18] The method is based on the experimental or theoretical rate-energy relation and the random lifetime assumption. The internal energy distribution for the dissociating $CH_2CF_2^{+\cdot}$ molecular ion has been estimated similarly.

Results and Discussion

The method to evaluate KERD from a MIKE profile has been described in detail previously.[20,21] Also, the MIKE profile for reaction (1) has been reported already together with the spectroscopic and thermodynamic constants needed for RRKM and phase space calculations.[18] Other relevant data such as the internal energy distribution for the dissociating $C_6H_6^{+\cdot}$ can be found from the same reference. It is to be noted, however, that the dissociating $C_6H_6^{+\cdot}$ molecular ion possesses the average excess energy of 1.03 eV at the transition state and that reaction (1) has the reverse barrier of 0.34 eV.[18] Figure 1 reproduces the experimental KERD for this reaction reported previously.[18] $n_{ex}(T)$ has been estimated in three different ways as described in the previous section and its contribution to the experimental KERD was subtracted *via* deconvolution. Two in-plane bending modes (800 cm^{-1}) and two out-of-plane bending modes (581 cm^{-1}) were taken as the four bending vibrations in the statistical adiabatic model estimation of $n_{ex}(T)$. The results are shown also in Figure 1. When $n_{ex}(T)$ estimated by RRKM calculation at the transi-
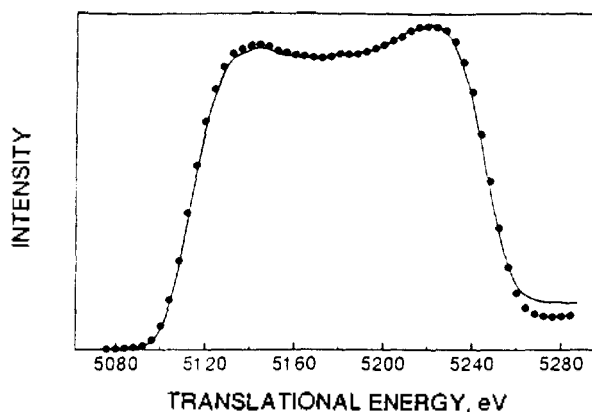

Figure 2. MIKE profile of reaction (2) occurring inside the cell floated at −1031 V. The solid curve represents the experimental data. KERD determined from this profile (experimental KERD, Figure 3) was used to regenerate the profile denoted by circles (●).
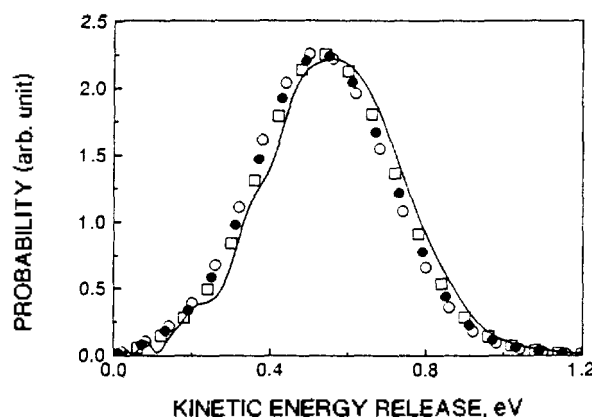

Figure 3. Solid line represents the experimental KERD in reaction (2). Symbols represent $n_r(T)$ estimated by the method described in the text. RRKM theory (□), the statistical adiabatic model (●), and the modified phase space calculation (○) have been used to estimate $n_{ex}(T)$ needed for the deconvolution of the experimental KERD.

tion state is used, the resulting $n_r(T)$ extends beyond 0.34 eV which is the total available energy for $n_r(T)$, namely the reverse barrier. This physically unrealistic result shows clearly that not only the reverse barrier and the translational energy along the reaction coordinate but also the energy stored in other degrees of freedom at the transition state is released as the relative translational energy of products. It is likely that the majority of this extra energy release comes from the energy stored in the modes which are coupled strongly with the reaction coordinate. $n_{ex}(T)$'s calculated by the statistical adiabatic model and the modified phase space calculation account for such an energy flow in two different ways. However, the close similarity between $n_r(T)$'s evaluated by the two methods shows that the details of the methods are not critical to the reliable estimation of $n_r(T)$. More importantly, the noticeable difference between the experimental KERD and the deconvoluted results points to the danger in disregarding the contribution from the excess

244 *Bull. Korean Chem. Soc.* **1994**, *Vol. 15, No. 3*

In Chul Yeh et al.

Table 1. Molecular parameters used for RRKM calculation and calculations of KERD in reaction (2)

A. Vibrational frequencies,[a] cm^{-1}

$CH_2CF_2^{+,b}$	3103	3060	1728	1414	1302	955
	926	803	611	590	550	438
$CHCF^{+,c}$						
+HF(TS)						
	3227	1974	1555[d,e]	1172	860[d,e]	833[d]
	723	605[d,e]	550	531	394	
$CHCF^{+,f}$	3355	2255	1055	578 (2)	367 (2)	
HF^g	4139					

B. Rotational constants, cm[-1]

$CH_2CF_2^{+,h}$	0.2834
$CHCF^{+,i}$	0.3238
HF^g	20.939

C. Polarizability, Å[3]

HF^j	2.46

[a]Numbers in the parentheses denote the degeneracies of vibrational modes. [b]Ref. 31. [c]Estimated values. [d]Vibrational Frequencies of transitional modes. [e]Bending vibrational frequencies used in the statistical adiabatic model calculation of KERD. [f]Ref. 32. [g]Ref. 33. [h]Ref. 34. [i]Ref. 35. [j]Ref. 36.

energy when the reverse barrier is not large.

Reaction (2) represents the case in the other extreme, namely the case when the reverse barrier is much larger than the excess energy. MIKE profile for reaction (2) occurring inside the cell maintained at -1031 V is shown in Figure 2. KERD evaluated from this MIKE profile is shown in Figure 3. The MIKE profile recalculated using KERD in Figure 3 is shown also in Figure 2. Except for the slight baseline mismatch at higher translational energy arising from interference, the experimental and regenerated profiles display excellent agreement. The internal energy distribution has been estimated by RRKM calculation. Molecular parameters used in RRKM calculation are shown in Table 1. Since reaction (2) is the dominant process in the unimolecular dissociation of $CH_2CF_2^+$, consideration for the competing reactions is not necessary. The critical energy for this reaction has been estimated to be 3.89 eV from the appearance and ionization energy data in Ref. 27. The average internal energy evaluated from the distribution is 3.97 eV. Hence, the dissociating parent ions possess the average excess energy of 0.08 eV at the transition state. Reaction (2) is endothermic by 2.67 eV as estimated by the difference in 0 K heats of formation between the products and the reactant.[28,29] Subtracting this from the forward critical energy, the reverse critical energy becomes 1.22 eV. Molecular parameters needed to evaluate $n_\alpha(T)$ according to the methods described in the previous section is also listed in Table 1. In the modified phase space calculation, the state sum for the linear-linear system was utilized.[30] The root-mean-square average of the rotational angular momentum over the thermal distribution was used.[18] Four vibrational modes at the transition state which evolve into the HF stretching vibration and the rotational and translational motions in the products were taken as the transitional modes. These modes are indicated in Table 1. Selection of the molecular parameters and the

transitional modes is somewhat arbitrary in this case. Since the excess energy is small, however, the final results were hardly affected by such selections.

$n_t(T)$'s obtained by deconvoluting the experimental KERD with $n_\alpha(T)$'s estimated in three different ways are shown also in Figure 3. Regardless of $n_\alpha(T)$'s used in the deconvolution, partitioning of the reverse barrier to the product relative translation has turned out to be nearly the same. Moreover, effect of the deconvolution is not significant as expected from the small excess energy compared to the reverse critical energy in reaction (2). This means that the experimental kinetic energy release distribution for a reaction with a large reverse barrier originates mostly from the reverse barrier and that the minor contribution from the excess energy can be reliably deconvoluted.

To summarize, a method has been developed to estimate the partitioning of the reverse critical energy to the product relative translation in unimolecular ion dissociation. Since $n_t(T)$ is intrinsic to the particular process, it will be useful in the study of reaction kinetics and mechanism for rearrangement reactions which usually exhibit significant reverse barriers. In addition, it is hoped that $n_t(T)$ thus obtained may form benchmark data which can be helpful in the development of statistical and dynamical theories for unimolecular reaction. The major problem in the present approach is found in the assumption that the contributions to the kinetic energy release from the two energy components can be dealt with separately and independently. Even though such an assumption is found frequently in the literature, its acceptability is not known. A theoretical guideline based on detailed dynamical investigation will be helpful in this regard. As for the results obtained for the reactions investigated, the experimental KERD originates almost entirely from the reverse barrier when the barrier is much larger than the excess energy. The minor contribution from the excess energy can be easily deconvoluted from the experimental data. On the other hand, proper deconvolution of the latter is important when the barrier is low. Even though the outcome was more or less model-dependent, a simple consideration for the evolution of the transitional modes as the system moves from the transition state to the product region seems to be adequate for the present purpose.

References

1. Aruman, E.; Wategaonkar, S. J.; Setser, D. W. *J. Phys. Chem.* **1991**, *95*, 1539.
2. Zamir, E.; Levine, R. D. *Chem. Phys.* **1980**, *52*, 253.
3. Wardlaw, D. M.; Marcus, R. A. *Advan. Chem. Phys.* **1988**, *70*, 231.
4. Marcus, R. A. *Chem. Phys. Lett.* **1988**, *144*, 208.
5. Chesnavich, W. J.; Bowers, M. T. *J. Am. Chem. Soc.* **1976**, *98*, 8301.
6. Chesnavich, W. J.; Bowers, M. T. *J. Chem. Phys.* **1977**, *66*, 2306.
7. Chesnavich, W. J.; Bowers, M. T. *J. Am. Chem. Soc.* **1977**, *99*, 1705.

The Crystal Structure of NaMg[Cr(ox)₃]·10H₂O

Bull. Korean Chem. Soc. 1994, Vol. 15, No. 3   245

8. Chesnavich W. J.; Bowers, M. T. *Prog. React. Kinet.* **1982**, *11*, 137.

9. Malinovich, Y.; Arakawa, R.; Haase, G.; Lifshitz, C. *J. Phys. Chem.* **1985**, *89*, 2253.

10. Jarrold, M. F.; Wagner-Redeker, W.; Illies, A. J.; Kirchner, N. J.; Bowers, M. T. *Int. J. Mass Spectrom. Ion Processes* **1984**, *58*, 63.

11. Bunn, T. L.; Bowers, M. T. *J. Phys. Chem.* **1988**, *92*, 1813.

12. Snodgrass, J. T.; Dunbar, R. C.; Bowers, M. T. *J. Phys. Chem.* **1990**, *94*, 3648.

13. Cooks, R. G.; Beynon, J. H.; Caprioli, R. M.; Lester, G. R. *Metastable Ions;* Elsevier: Amsterdam, 1973; p 104.

14. Levsen, K. *Fundamental Aspects of Organic Mass Spectrometry;* Verlag Chimie: Weinheim, 1978; p 134.

15. Marcus, R. A. *J. Chem. Phys.* **1975**, *62*, 1372.

16. Worry, G.; Marcus, R. A. *J. Chem. Phys.* **1977**, *67*, 1636.

17. Parson, J. M.; Lee, Y. T. *J. Chem. Phys.* **1972**, *56*, 4658.

18. Yeh, I. C.; Kim, Y. H.; Kim, M. S. *Chem. Phys. Lett.* **1993**, *207*, 487.

19. Sloan, J. J. *J. Phys. Chem.* **1988**, *92*, 18.

20. Yeh, I. C., Kim, M. S. *Rapid Commun. Mass Spectrom.* **1992**, *6*, 115.

21. Yeh, I. C.; Kim, M. S. *Rapid Commun. Mass Spectrom.* **1992**, *6*, 293.

22. Kim, Y. H.; Kim, M. S. *Rapid Commun. Mass Spectrom.* **1991**, *5*, 25.

23. Brigham, E. O. *The Fast Fourier Transform and Its Applications;* Prentice-Hall: London, 1988; p 204, p 345.

24. Robinson, P. J.; Holbrook, K. A. *Unimolecular Reactions;* Wiley-Interscience: New York, 1972; p 64.

25. Forst, W. *Theory of Unimolecular Reactions;* Academic Press: New York, 1973; p 28.

26. Chesnavich, W. J.; Bowers, M. T. *J. Phys. Chem.* **1979**, *83*, 900.

27. Reinke, D.; Kraessig, R.; Baumgärtel, H. Z. *Naturforsch.* **1973**, *28a*, 1021.

28. Lias, S. G.; Bartmess, J. E.; Liebman, J. F.; Holmes, J. L.; Levin R. D.; Mallard, W. G. *J. Phys. Chem. Ref. Data* **17** Suppl. 1, **1988**,*81*, 83, 604.

29. Traeger, J. C.; McLoughlin, R. G. *J. Am. Chem. Soc.* **1981**, *103*, 3647.

30. Grice, M. E.; Song, K.; Chesnavich, W. J. *J. Phys. Chem.* **1986**, *90*, 3503.

31. Smith, D. C.; Nielsen, J. R.; Claassen, H. H. *J. Chem. Phys.* **1950**, *18*, 326.

32. Hunt, G. R.; Wilson, M. K. *J. Chem. Phys.* **1961**, *34*, 1301.

33. Herzberg, G. *Molecular Spectra and Molecular Structure, I. Spectra of Diatomic Molecules;* D. Van Nostrand Company: 2nd end; New York, p 536.

34. Lafferty, W. J.; Sattler, J. P.; Worchesky, T. L.; Ritter, K. J. *J. Mol. Spectrosc.* **1981**, *87*, 416.

35. Jones, H.; Rudolph, H. D. Z. *Naturforsch.* **1979**, *34a*, 340.

36. Hirschfelder, J. O.; Curtiss, C. F.; Bird, R. B. *Molecular Theory of Gases and Liquids;* John Wiley & Sons: New York, 1954; p 950.

The Crystal and Molecular Structure of Sodium Magnesium Tris(oxalato)Chromate(III) Decahydrate, NaMg[Cr(ox)₃]·10H₂O

Jung-Sun Suh, Jung-Yup Shin, Cheonho Yoon, Kyu-Wang Lee
Il-Hwan Suh*, Jin-Ho Lee*, Bo-Young Ryu*, and Sung-Su Lim*

Department of Chemistry, Myongji University Yongin, Kyonggi-do 449-728
*Department of Physics, Chungnam National University, Taejon 305-764

NaMg[Cr(C₂O₄)₃]·10H₂O crystallizes in the trigonal space group P$\bar{3}$c1, with $a=b=16.969(3)$, $c=12.521(3)$ Å, $\alpha=\beta=90°$, $\gamma=120°$, $\rho=1.734$ gcm^{-3}, $\mu=6.46$ cm^{-1}, $Z=6$. Intensities for 1062 unique reflections were measured on a four-circle diffractometer with Mo Kα radiation ($\lambda=0.71069$ Å). The structure was solved by direct methods and refined to a final ωR value of 0.084. X-ray crystal structure showed that magnesium ion appears to be occupied over two sites with the occupancy ratio of 2:1. The crystal possesses 10 water molecules instead of previously estimated 9 water molecules.

Introduction

Even though the magnetic and electronic properties of [Cr(ox)₃]³⁻ [ox=(C₂O₄)²⁻] have been extensively studied under the guidelines of conventional ligand field theory, the results are not always in agreement.[1⁻3] The type of space group has been controversially discussed for the interpretation of EPR and PMR results.[4] Band assignments in the sharp lines

arising from t_{2g}^3 intraconfigurational transition are still controversial.

Mortensen reported 20 cm⁻¹ splitting of ²E_g line in NaMg salt,[2] while Coleman observed large variance of ²E_g splittings (from 2 to 115 cm⁻¹) which have been attributed to the degree of hydration and the effects of the counter ion in a molecule.[5] Recently Schönherr *et al.* assigned the ²E_g lines split by 2-3 cm⁻¹ which was rationalized by the angular over-